RevMexAA (Serie de Conferencias), **1**, 149-156 (1995)

SIGNATURES OF CONTRACTING MOLECULAR CORES WITH LOW-MASS STAR FORMATION

José M. Torrelles, José F. Gómez

Instituto de Astrofísica de Andalucía, CSIC, Ap. Correos 3004,
C/ Sancho Panza S/N, E-18080 Granada, Spain

and

Guillem Anglada

Departament d'Astronomia i Meteorologia, Universitat de Barcelona,
Av. Diagonal 647, E-08028 Barcelona, Spain

RESUMEN

En este artículo se resumen diversos trabajos teóricos y observacionales encaminados a predecir y detectar signos de colapso gravitatorio en núcleos moleculares con formación de estrellas de baja masa, usando para ello los perfiles de líneas moleculares. También se discuten dos casos publicados en la literatura muy recientemente, HH 1-2 y HL Tau, en donde los datos obtenidos acerca de la cinemática general de la región se interpretan en términos de movimientos de contracción, resueltos tanto espectral como espacialmente.

ABSTRACT

In this paper we summarize several theoretical and observational efforts aimed to predict and detect collapse signatures in molecular cores with low-mass star formation, using molecular line profiles. We also discuss two recently reported cases, HH 1-2 and HL Tau, where spatially and spectrally resolved contracting motions have been inferred from the data of the general kinematics of the region.

Key words: **ISM: JETS AND OUTFLOWS — ISM: MOLECULES — LINE: PROFILES — STARS: MASS LOSS — STARS: PRE-MAIN-SEQUENCE**

1. INTRODUCTION

It is now well known that strong mass outflows are one of the first observable signatures associated with the earliest stages of stellar evolution (Rodríguez et al. 1982, Lada 1985). Observations of molecular tracers of high-density gas [$n(H_2) \geq 10^4$ cm^{-3}] (e.g., NH_3, CS) have shown that the young stellar objects (YSOs) that power these outflows are almost always found embedded in high-density molecular gas (practically a one-to-one association; Torrelles et al. 1983, 1986; Anglada et al. 1989). Furthermore, several observational studies have shown that molecular clouds present gas density gradients, with stars forming in the densest portion of the cloud cores (c.f., Snell et al. 1984). This indicates that gravitational collapse of the molecular core has inevitably occurred at some point of the star forming process.

However, contrary to outflow motions in star formation, which are easily observable, the detection of contracting gas in molecular cores continues to be a long-standing observational problem (star whose energy is produced purely by accretion is sometimes referred to as the *Holy Grail* of star formation). In this sense, although a number of observational studies reporting contracting motions in both high and low-mass molecular cores have been published (c.f., Ho & Haschick 1986; Zhou et al. 1993), the interpretation of the kinematic features of these molecular cores in terms of collapse is not as straightforward as for outflows. As many authors have already pointed out, one of the difficulties for detecting contracting motions in molecular cores comes

from the fact that both collapse and outflow in star forming regions can coexist, according to theory (c.f., Shu, Adams, & Lizano 1987). Given the ubiquity of outflows in regions of star formation, these could mask and make more difficult the detection of contracting motions in cloud cores.

In order to distinguish unambiguously infall from outflow it is necessary to be able to discriminate whether the redshifted emission comes from material which is in front of or behind the blueshifted material (that is, in the case of infalling motions the receding material will be in the part of the cloud nearest the observer and the approaching material will be in the background side, while the opposite is true for outflow). Several procedures have been used in order to distinguish the emission from the front side of the core from that coming from the back side: *(a)* redshifted or blueshifted absorption lines against a bright continuum background provided by an embedded HII region (the molecular line from the front side of the core is seen in absorption against a compact embedded HII region, while the line from the back side of the core is seen in emission; Ho & Haschick 1986); *(b)* relative orientation between jet and disk (the 3-D orientation of a disk can be inferred knowing the radial velocities of the jet assuming that it emerges perpendicularly to the plane of the disk; Torrelles et al. 1993, 1994, Hayashi et al. 1993, see § 3); *(c)* obscuration of optical emission by the foreground gas (the optical jet emission is obscured by the foreground side of a molecular disk; Torrelles et al. 1994, see § 3); *(d)* optically thick line emission in clouds with temperature gradients (line profiles are asymmetric when optically thick blueshifted emission originates in regions with a different excitation temperature from that of the corresponding redshifted emission; Anglada et al. 1987, 1991, Keto 1991, Walker, Carlstrom, & Bieging 1993, Zhou et al. 1993, see § 2). The first three procedures require that the emission is spatially resolved, while the fourth one can be applied even if it is not.

In this paper, we will concentrate on several theoretical and observational efforts aimed to predict and detect collapse signatures in molecular cores with low-mass star formation using molecular line profiles (§ 2). We will also discuss two recently reported cases, HH1-2 and HL Tau, where the kinematics of the molecular gas in the cores is spatially resolved, and whose emission distribution pattern is consistent with contracting motions (§ 3).

2. THE SPECTRAL HALLMARK OF CONTRACTING PROTOSTELLAR CLOUDS: OBSERVATIONAL EVIDENCES OF COLLAPSE?

The problem of how to discriminate, from line profiles, between infall and outflow in protostellar cores was analyzed by Anglada et al. (1987). The main result of that study was that, for those molecular transitions whose emission is optically thick, protostellar collapse will produce asymmetric line profiles, with the blue wing stronger than the red wing.

To reach this conclusion, Anglada et al. (1987) considered a cloud with spherically symmetric velocity and temperature distributions described by power laws, $V \propto r^{-\alpha}$, $T \propto r^{-\beta}$ ($\alpha > 0$, β arbitrary). Provided the velocity increases toward the center of the cloud (that is, $\alpha > 0$; this includes both accelerating infall and decelerating outflow), the points with the same projected velocity on the line of sight define *closed* surfaces as those illustrated in Fig. 1. In general, a line of sight intercepts a given isovelocity surface at two points. Then, if the emission is optically thick, the emission observed at a given velocity is coming from the side of its respective isovelocity surface facing the observer (thick line in Fig. 1), while the emission from the rear portion of the isovelocity surface (thin line in Fig. 1) will be hidden, and not observable. It should be noted that, if the velocity is constant along the cloud ($\alpha = 0$) or decreases toward its center ($\alpha < 0$), the isovelocity surfaces will be *open* surfaces, and all the points will be observable, since along a given line of sight they all have different projected velocities.

Assuming that the emission is not angularly resolved by the telescope, Anglada et al. (1987) obtained an analytical expression for the wing line profile of an optically thick molecular transition originated in such a cloud. The line profile depends on the velocity and temperature distributions, but the main result is that if the temperature distribution is not uniform along the cloud ($\beta \neq 0$), the line profile is asymmetric, and the ratio of antenna temperatures at two velocities that are symmetric with respect to the line center is given by

$$\frac{T_A(z<0)}{T_A(z>0)} = 1 - \frac{\beta}{2}(1+\alpha)^{-(\beta-2)/2\alpha}. \quad (1)$$

The reason of this asymmetry can be easily understood by looking at Fig. 1, and taking into account that, for optically thick emission, only the side of the isovelocity surfaces closer to the observer will be visible (thick line in Fig. 1). For infall motions, the blueshifted emission comes from points located closer to the center of the cloud (and thus, hotter, if the temperature increases inward) than the corresponding redshifted emission. Thus,

the blue wing will be stronger than the red wing. The opposite is true for outflow (provided the excitation temperature increases inward). Since for gravitational collapse both velocity and temperature are expected to increase toward the center of the cloud, this characteristic asymmetry of the wing line profile was considered as *the spectral hallmark* of protostellar collapse. As pointed out by Anglada et al. (1987), this result is valid for any molecular transition for which the observed emission is optically thick (for optically thin species the lines will be symmetric and can be used to define the central velocity of the emission).

This asymmetry should not be confused with that discussed by Leung & Brown (1977), which is not applicable to the cases (either outflow or infall) discussed here. The asymmetries discussed by Leung & Brown (1977) apply when the systematic velocities are smaller than the thermal and turbulent broadening, and the isovelocity surfaces are open ($\alpha \leq 0$), which is not the case here, as it was discussed before (note, also, that the asymmetry in the case of expansion only appears at positions displaced from the center of the cloud). Other radiative transfer effects that result in asymmetric profiles for velocity fields with open isovelocity surfaces, act symmetrically on both sides of the resulting line profile when applied to velocity fields with closed surfaces (see the discussion in Anglada et al. 1987, and references therein). However, it is worth noting that, for line profiles toward the center of the cloud, all these cases result in blueshifted emission stronger than the redshifted emission, for infall motion and temperatures increasing inward. So, the infall signature is not expected to be mimicked by outflow motions.

Anglada et al. (1987) applied their results to the "main accretion phase" of the Larson (1972) model, when the cloud is infalling almost in free fall, and the velocity, temperature and density of the collapsing cloud are described by power laws of the form $V \propto r^{-1/2}$, $T \propto r^{-1/2}$, $\rho \propto r^{-3/2}$. It should be noted that, even though the initial conditions are quite different, the velocity and density distributions in the main accretion phase of the numerical model of Larson (1972) (not be confused with the so-called Larson-Penston flow, in which the distributions scale differently) are virtually the same as in the infall region of the analytical solution obtained by Shu (1977) (the model of Shu 1977 does not provide a temperature distribution). In order to avoid the emission from the ambient cloud and since the emission at the lowest velocities could start to be angularly resolved, only the emission in the wings was calculated. In this way, the ratio between blueshifted and redshifted intensities is ~2, as it can be derived from Eq. (1). An additional signature of protostellar collapse is that the asymmetric line profile was estimated to be originated only in a region of small angular size (a few arcsec for a nearby cloud). To illustrate the detectability with large radio telescopes in the mm wavelength range, it was calculated the expected CO spectrum at the time when one half solar mass is accreted. This spectrum is shown in Fig. 1.

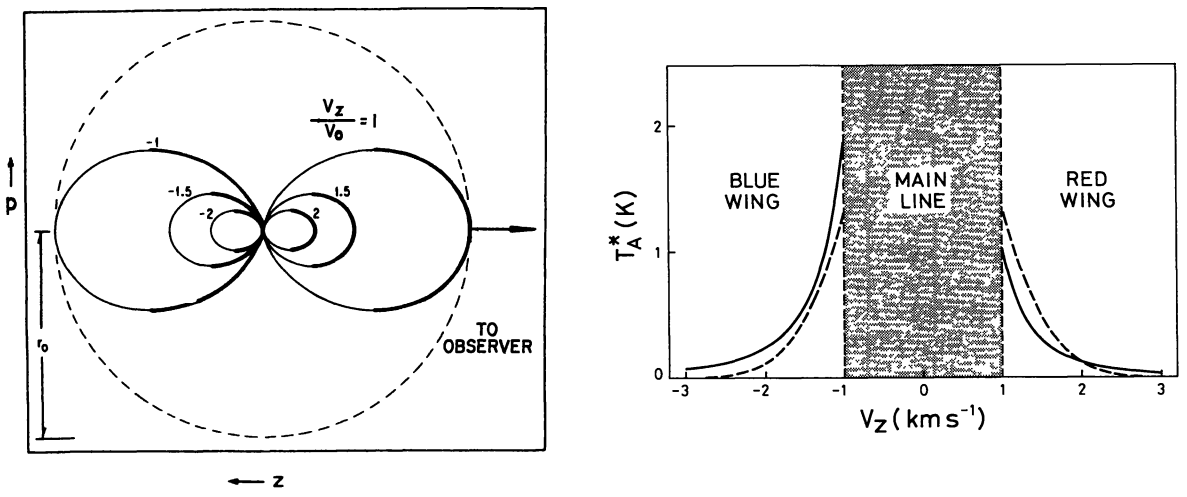

Fig. 1.— *(Left)* Contours of equal line-of-sight projected velocity, for a spherically symmetric velocity field such that velocity increases toward the center. The values of the velocities indicated correspond to the case of infall; for the case of outflow the contours would be the same, but the sign of the velocity would be the opposite. The thick line indicates the observable side for optically thick emission. *(Right)* Expected wing line profile for a nearby contracting protostellar core at the time when one half of a solar mass has been accreted (solid line), as observed with a large single-dish radio telescope. A Gaussian profile (dashed line) is shown as a comparison. (Figure from Anglada et al. 1987).

Anglada et al. (1991) studied the influence of the angular resolution of the instrument on the observed molecular line profiles. Provided the emission is optically thick enough, for protostellar collapse the blue wing was always found to be stronger than the red wing. As the angular resolution increases, the low velocity emission is progressively resolved, the blue wing flattens, and a clear dip appears at the low velocity end of the red wing, increasing the asymmetry of the line (see Fig. 3 of Anglada et al. 1991). For very high angular resolution observations ($\leq 1''$) additional signatures allowing to distinguish between infall and outflow were found in the spatial distribution of the emission at different velocities. In the case of infall, in the maps of the blueshifted emission, the intensity of the emission increases sharply toward the center of the field; in contrast, in the maps of the redshifted emission, a smooth decrease in the intensity occurs near the center. In addition, the size of the emitting region decreases as the velocity increases (see Fig. 6 of Anglada et al. 1991). Unfortunately, the sensitivity and angular resolution of the present interferometers is insufficient to detect these signatures in the spatial distribution of the emission. However, we think that it could be detectable with the next generation of interferometers working at mm and sub-mm wavelengths, which will provide angular resolutions of $\leq 1''$. The influence of cloud rotation in the emergent line profile and the problem of detection of infall toward binary systems have been taken into account in a recent analysis by Walker, Narayanan, & Boss (1994).

Observational evidence for the spectral hallmark discussed before, may come from the results of Walker, Carlstrom, & Bieging (1993) in the IRAS 16293−2422 cloud core and those of Zhou et al. (1993) in B335. In fact, Walker et al. (1993) report asymmetries in the CS ($J = 2 \rightarrow 1$) line wings observed toward the source 1629a, with the blue wing being two times stronger than the red wing (the ratio predicted by Eq. 1). On the other hand, Zhou et al. (1993) make a very detailed observational study of the B335 cloud in several molecular transitions, obtaining asymmetric line profiles with the blueshifted emission brighter than the redshifted emission. Zhou et al. (1993) considered in detail the excitation of the H_2CO and CS molecules and calculate the whole line profile (including the low velocities which are affected by the ambient gas), using the velocity and density distributions of the "inside-out" model of Shu (1977) and the temperature distribution obtained by Zhou et al. (1990) from the spectral distribution of the dust continuum emission. Zhou et al. (1993) obtained a good fit to the observed spectra of the different transitions, deriving the physical parameters of the infalling cloud, according to the model of Shu (1977). Zhou et al. (1993) also considered alternative models (foreground absorption, static core, rotation, expansion, etc.), showing that none of these can explain the line profiles observed in the B335 cloud. Similar studies based on the line profiles of $C^{18}O$ and H_2CO have been extended by Zhou et al. (1994) to other molecular cores, finding signs of collapse in L1527.

All these observational results are very promising, and further observations with higher angular resolution and sensitivity, in order to detect emission at higher velocities, will certainly be very useful to complete the analysis. Clearly, intensive observations with the next generation of radio interferometers (see Ho 1995 in these Proceedings), which will provide angular resolutions of $\leq 1''$ and will start to resolve spatially the emission, could provide a more conclusive test for these collapse interpretations.

3. THE HH1-2 AND HL TAU MOLECULAR CORES: SPATIALLY AND SPECTRALLY RESOLVED CONTRACTING MOTIONS?

In addition, there are other cases of molecular cores with low-mass star formation where contracting motions have been inferred, but in this case based on the general kinematics of the region, including both outflow and cloud core motions, rather than through radiative transfer models of the expected molecular line profiles (see § 2). These are the cases of the HH1-2 (Torrelles et al. 1992, 1993, 1994) and HL Tau (Hayashi, Ohashi, & Miyama 1993) molecular cores. In both regions, the important key to conclude contracting motions has been the comparison between the velocity field of the optical jet associated with the YSO and the velocity field of the molecular core.

3.1. HH1-2

Ammonia observations at 1.3 cm carried out by Torrelles et al. (1985) with the 37-m telescope of the Haystack Observatory (beam $\simeq 1'.4$) toward this region showed an elongated ($\simeq 3' \times 2'$; 0.40×0.27 pc at a distance of 460 pc) high-density molecular condensation centered on VLA 1 (Pravdo et al. 1985, Rodríguez et al. 1990), the exciting source of the Herbig-Haro (HH) objects 1 and 2. This condensation is oriented perpendicular to the optical bipolar outflow traced by the HH1 and HH2 objects, which are moving in opposite directions almost on the plane of the sky (Herbig & Jones 1981). These single-dish ammonia observations also showed that toward the central positions the ammonia lines split into two velocity components separated by $\simeq 2$ km s^{-1}. Torrelles et al. (1992, 1993, 1994) have recently completed a mosaic analysis combining five fields of VLA-D ammonia

observations (beam $\simeq 4''$), recovering the extended emission observed with the Haystack telescope. Torrelles and coworkers resolve the two velocity components of ammonia observed with single-dish into two parallel elongated structures of 0.4 pc in size, moving at $V_{LSR} \simeq 8.1$ and 10.6 km s^{-1}, whose major axes are almost perpendicular to the HH1-2 outflow and displaced $20''$ northwest and $10''$ southeast of VLA 1, respectively (Fig. 2). This pattern of ammonia emission is analogous to that found in the HH1-2 outflow, with HH1 blueshifted to the northwest of VLA 1 and HH2 redshifted to the southeast (Schwartz 1983). A very important observational key on the HH1-2 system, provided by the ammonia mosaic analysis, is that the [SII] emission related to the HH1-2 bipolar outflow seems to emerge from the edges of the southeastern elongated ammonia structure ($V_{LSR} \simeq 10.6$ km s^{-1}), while [SII] emission is observed superposed on the northwestern elongated structure ($V_{LSR} \simeq 8.1$ km s^{-1}) (Fig. 2). This result indicates that the elongated high-density molecular structure moving at $V_{LSR} \simeq 10.6$ km s^{-1} is obscuring the optical [SII] emission from the bipolar outflow of VLA 1 and is consequently in the foreground with respect to the elongated structure moving at $V_{LSR} \simeq 8.1$ km s^{-1}.

Torrelles and coworkers consider two possible scenarios to explain the morphology and kinematics of the two parallel elongated high-density molecular structures: *the low-velocity molecular outflow scenario*, and *the contracting interstellar molecular toroid scenario.*

The low-velocity molecular outflow scenario. In this scenario, since the spatial and velocity pattern of the elongated structures is analogous to the velocity pattern of the HH1 and HH2 optical outflow (blueshifted motions to the northwest and redshifted motions to the southeast), one could argue that both elongated structures are part of a molecular outflow generated by the same wind that is producing the HH1-2 outflow. However, as noted above, the southeastern elongated structure, which is redshifted with respect to the northwestern one, is located in the foreground. This strongly argues against the hypothesis that the general kinematics and spatial distribution of the two elongated structures are part of a molecular outflow produced by VLA 1.

The contracting interstellar molecular toroid scenario. In this scenario, it is proposed that the southeastern and northwestern elongated structures represent the two halves of an interstellar molecular toroid ($\simeq 0.4$ pc in size) seen almost edge-on, with an orientation similar to the proposed circumstellar disk ($\leq 10^3$ AU in size) that should be responsible for the collimation of the radio jet of VLA 1 (Rodríguez et al. 1990). In this case, the radial velocities would represent contracting motions. A simplified schematic diagram of this contracting interstellar toroid scenario is presented in Fig. 3 (Plate 2). The four main points argued by Torrelles and coworkers to favor this scenario in HH1-2 are: (1) Intermediate velocities between the two halves of the structure are found at their northeastern and southwestern ends, as expected for a contracting toroid (see Fig. 4). (2) As argued in Torrelles et al. (1993), "if we adopt the geometry where the central dense structure is perpendicular to the HH1-2 outflow, with an orientation similar to that of the possible collimating circumstellar disk, then the blueshifted motions of HH1 with respect to HH2 argues that the southeastern side of the central ammonia structure is in the foreground with respect to the northwestern side. The redshifted motion of the foreground side then argues that the radial motion could be contraction and not expansion". This argument is consistent with the *independent* result obtained by comparing the spatial distribution of the two elongated ammonia structures and the [SII] emission of the HH1-2 system, implying that the southeastern side is in the foreground with respect to the northwestern one (see above; Fig. 2). (3) The mass of the toroid ($\simeq 40$ M$_\odot$, adopting an abundance $X_{NH_3} = 10^{-8}$) is enough to produce by itself contracting motions of $\simeq 1$ km s^{-1} at scales of $\simeq 0.2$ pc. Furthermore, the southeastern elongated structure presents a velocity gradient along its minor axis, with the highest velocities toward VLA 1 (see Fig. 4). This is consistent with contracting motions around VLA 1. (4) VLA 1 is located almost in between the two elongated ammonia structures, which is consistent with the idea of a toroid surrounding the exciting source (Figs. 2 and 3 [Plate 2]).

Although the contracting interstellar toroid scenario is not a *unique* model to explain the distribution of the high-density molecular gas in the region (for example, two elongated colliding clouds with velocities $V_{LSR} \simeq 8.1$ and 10.6 km s^{-1}, respectively, cannot be discarded), we consider this scenario as the one that can explain in an easier way most of the observed characteristics of the HH1-2 region.

Very recently, Stapelfeldt (1995) has reported with the OVRO interferometer a C^{18}O structure around VLA 1, with a size of $7''.6 \times 4''.8$ elongated along a P.A. $= 67°$, therefore almost parallel to the interstellar ammonia elongated structures, but a factor $\simeq 20$ smaller. The C^{18}O structure has a velocity $V_{LSR} \simeq 10.4$ km s^{-1}, similar to the velocity of the southeastern elongated ammonia structure. This is consistent with the result obtained by Torrelles et al. (1994) in the sense that VLA 1 is found to be spatially closer to the southeastern elongated structure than to the northwestern one, since the observed temperature of the molecular gas in that structure is higher in its neighborhood. The detection of the small C^{18}O structure ($\simeq 3500 \times 2200$ AU; Stapelfeldt 1995) is very important because it could be related to the circumstellar collimating disk around VLA 1 proposed by Rodríguez et al. (1990). The fact that the VLA ammonia mosaic analysis did not distinguish this small structure

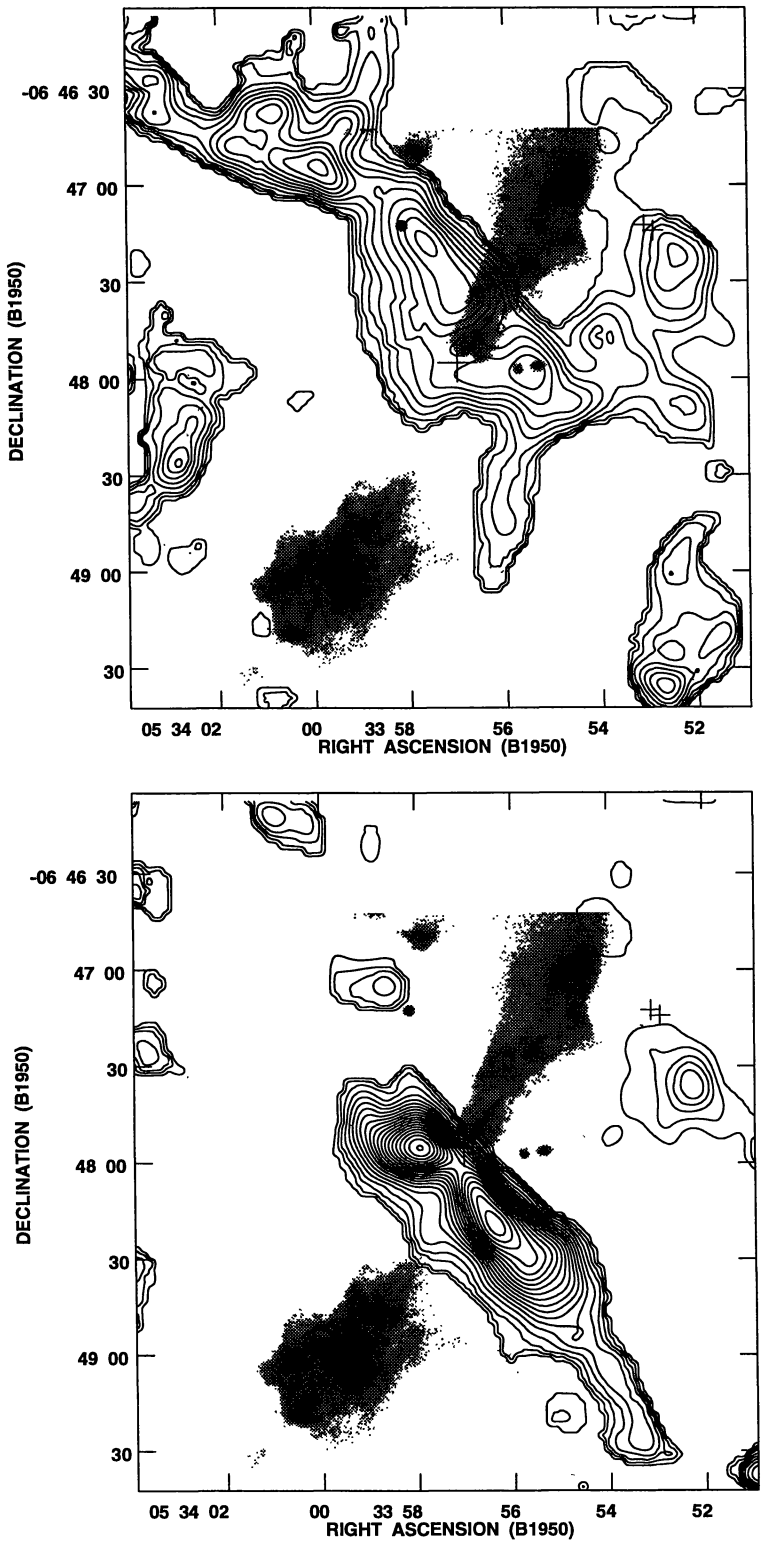

Fig. 2.— $NH_3(1,1)$ main line in the velocity ranges *(up)* $[V_{LSR}/\mathrm{km\ s^{-1}}] = [7.1,9.0]$ and *(down)* $[V_{LSR}/\mathrm{km\ s^{-1}}] = [9.6,11.5]$. Superposed to these contour maps there is a logarithmic gray-scale map of the [SII] $\lambda\lambda$ 6716+6731 line emission of the HH 1-2 system. The position of VLA 1 is indicated by a large cross. Small crosses indicate the positions of two radio continuum sources in the region. (Figure from Torrelles et al. 1994).

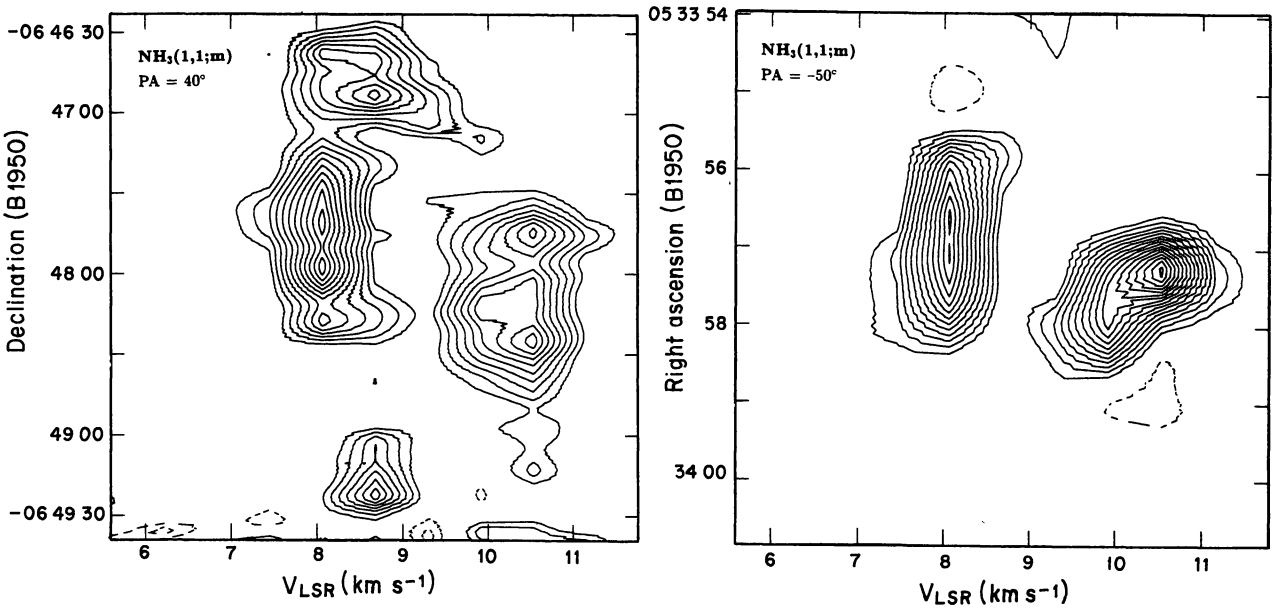

Fig. 4.— Spatial-velocity diagrams of the $NH_3(1,1)$ main line along *(left)* the direction with P.A. = 40°(coinciding with the direction of the major axes of the elongated structures), through the position of VLA 1, and *(right)* along a perpendicular direction (P.A. = –50°), through VLA 1. (Figure from Torrelles et al. 1994).

around VLA 1 (Torrelles et al. 1994) could be either because the $C^{18}O$ is more sensitive to the molecular gas with relatively high temperatures than the (1,1) and (2,2) ammonia transitions used for the mosaic analysis, or due to depletion of the ammonia gas within few hundred AU from VLA 1, as suggested in other molecular cores of low-mass star formation (c.f., Wootten 1994).

In summary, the HH1-2 system represents a remarkable case where the star formation processes seem to have originated several flattened structures surrounding the YSO (VLA 1), with sizes of $\simeq$ 0.4 pc (the interstellar toroid), $\simeq$ 3000 AU (the $C^{18}O$ structure), and $\leq 10^3$ AU (the collimating circumstellar disk of the VLA 1 radio jet), all of them having almost the same orientation (*disks inside disks*). Finally, HH1-2 would be a case where the idea that inflow and outflow are taking place simultaneously in YSOs is supported.

3.2. HL Tau

This source exhibits similar characteristics to those shown by HH1-2. Interferometric observations of ^{13}CO (Sargent & Beckwith 1991) revealed a disk of $\simeq$ 3000 AU in size, whose major axis is oriented nearly perpendicular to the associated optical jet (Mundt, Ray, & Bürke 1988; but see Rodríguez et al. 1994 for images of the disk and jet with 50 AU of resolution). Hayashi et al. (1993), using the Nobeyama Millimeter Array, noted that the ^{13}CO emission at the northeastern part of the disk is blueshifted with respect to its major axis, while the southwestern part is redshifted. Since the northeastern part of the optical jet is blueshifted with respect to the southwestern part (Mundt et al. 1988), Hayashi and coworkers conclude that the southwestern part of the ^{13}CO disk is in the foreground with respect to the northeastern one, with the ^{13}CO velocities representing contracting motions within a scenario similar to that represented in Fig. 3 (Plate 3) for HH1-2.

G.A. acknowledges financial support from CIRIT de Catalunya (Spain). G.A., J.F.G. and J.M.T. are partially supported by DGICYT grant PB92-0900 (Spain).

REFERENCES

Anglada, G., Rodríguez, L. F., Cantó, J., Estalella, R., & López, R. 1987, A&A, 186, 280
Anglada, G., Rodríguez, L. F., Torrelles, J. M., Estalella, R., Ho, P. T. P., Cantó, J., López, R., & Verdes-Montenegro, L. 1989, ApJ, 341, 208
Anglada, G., Estalella, R., Rodríguez, L. F., Cantó, J., & López, R. 1991, A&A, 252, 639

Hayashi, M., Ohashi, N., & Miyama, S. M. 1993, ApJ, 418, L71
Herbig, G. H., & Jones, B. F. 1981, AJ, 86, 1232
Ho, P. T. P. 1995, in Disks, Outflows and Star Formation, ed. S. Lizano & J. M. Torrelles, RevMexAASC, 1, 363
Ho, P. T. P., & Haschick, A. D. 1986, ApJ, 304, 501
Keto, E. 1991, ApJ, 371, 163
Lada, C. J. 1985, ARA&A, 23, 267
Larson, R. B. 1972, MNRAS, 157, 121
Leung, C. M., & Brown, R. L. 1977, ApJ, 214, L73
Mundt, R., Ray, T. P., & Bürke, T. 1988, ApJ, 333, L69
Pravdo, S. H., Rodríguez, L. F., Curiel, S., Cantó, J., Torrelles, J. M., Becker, R. H., & Sellgren, K. 1985, ApJ, 293, L35
Rodríguez, L. F., Cantó, J., Torrelles, J. M., Gómez, J. F., Anglada, G., & Ho, P. T. P. 1994, ApJ, 427, L103
Rodríguez, L. F., Carral, P., Ho, P. T. P., & Moran, J. M. 1982, ApJ, 260, 635
Rodríguez, L. F., Ho, P. T. P., Torrelles, J. M., Curiel, S., & Cantó, J. 1990, ApJ, 352, 645
Sargent, A., & Beckwith, S. V. W. 1991, ApJ, 382, L31
Schwartz, R. D. 1983, RevMexAA, 7, 27
Shu, F. H. 1977, ApJ, 214, 488
Shu, F. H., Adams, F. C., & Lizano, S. 1987, ARA&A, 25, 23
Snell, R. L., Mundy, L. G., Goldsmith, P. F., Evans II, N. J., & Erickson, N. R. 1984, ApJ, 276, 625
Stapelfeldt, K. R. 1995, in preparation (poster presented at this conference on Circumstellar Disks, Outflows and Star Formation; Cozumel, México, November 1994)
Torrelles, J. M., Cantó, J., Rodríguez, L. F., Ho, P. T. P., & Moran, J. M. 1985, ApJ, 294, L117
Torrelles, J. M., Gómez, J. F., Ho, P. T. P., Anglada, G., Rodríguez, L. F., & Cantó, J. 1993, ApJ, 417, 655
Torrelles, J. M., Gómez, J. F., Ho, P. T. P., Rodríguez, L. F., Anglada, G., & Cantó, J. 1994, ApJ, 435, 290
Torrelles, J. M., Ho, P. T. P., Moran, J. M., Rodríguez, L. F., & Cantó, J. 1986, ApJ, 307, 787
Torrelles, J. M., Rodríguez, L. F., Cantó, J., Anglada, G., Gómez, J. F., Curiel, S., & Ho, P. T. P. 1992, ApJ, 396, L95
Torrelles, J. M., Rodríguez, L. F., Cantó, J., Carral, P., Marcaide, J. M., Moran, J. M., & Ho, P. T. P. 1983, ApJ, 274, 214
Walker, C. K., Carlstrom, J. E., & Bieging, J. H. 1993, ApJ, 402, 655
Walker, C. K., Narayanan, G., Boss, A. P. 1994, ApJ, 431, 767
Wootten, A. 1994, in Circumstellar Matter, ed. G. Watt, in press
Zhou, S., Evans II, N. J., Butner, H. M., Kutner, M. L., Leung, C. M., & Mundy, L. G. 1990, ApJ, 363, 168
Zhou, S., Evans II, N. J., Kömpe, C., & Walmsley, C. M. 1993, ApJ, 404, 232
Zhou, S., Evans II, N. J., Wang, Y., Peng, R., & Lo, K. Y. 1994, ApJ, 433, 131

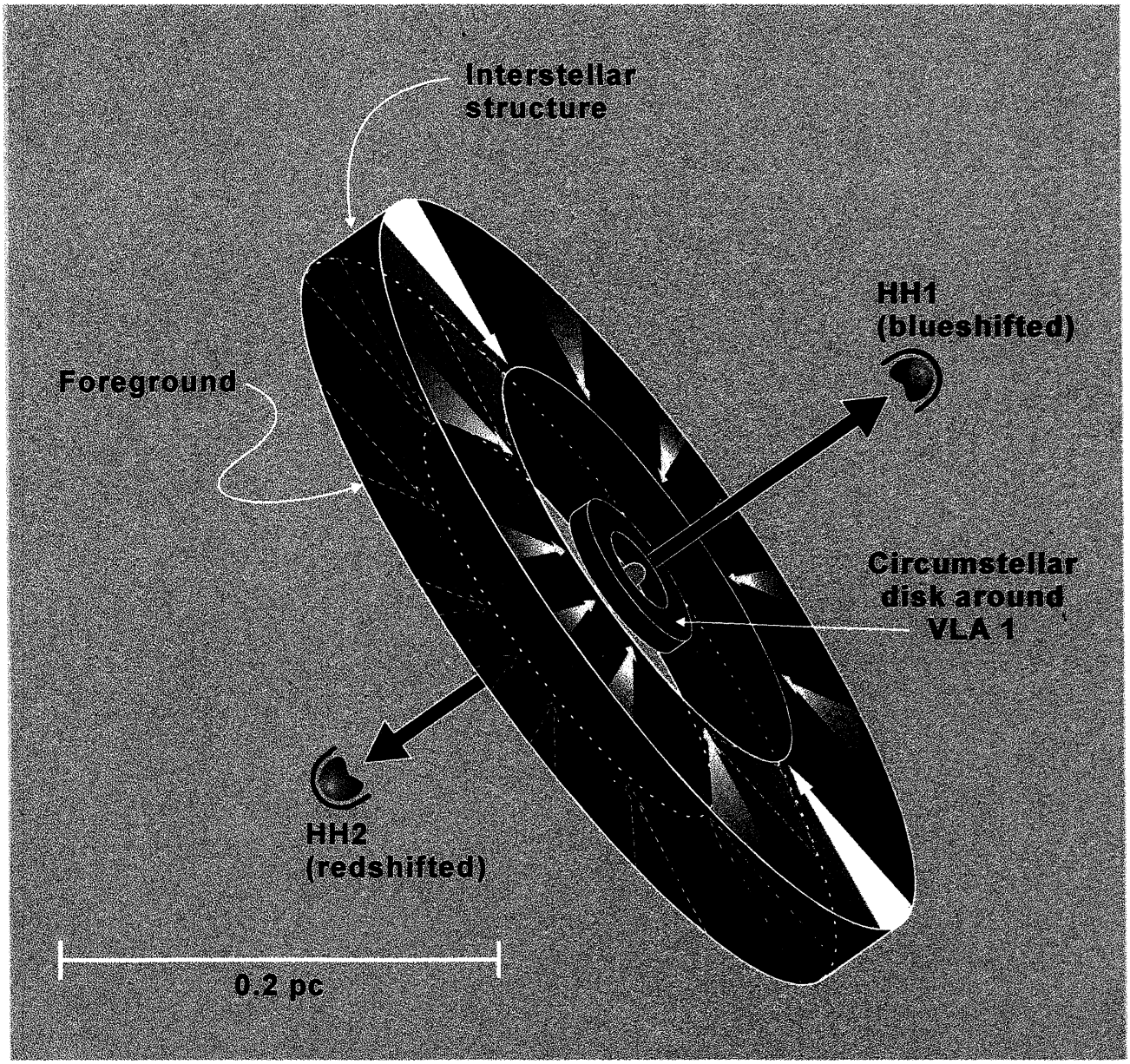

Fig. 3.— Schematic representation of the contracting interstellar toroid scenario in HH 1-2.

TORRELLES, GÓMEZ, & ANGLADA (see page 149)